Strojniški vestnik - Journal of Mechanical Engineering 54(2008)9, 628-638
UDC 658.34.17

Paper received: 04.07.2007
Paper accepted: 07.07.2008

A Device for Simulating the Thermoregulatory Responses of the Foot: Estimation of Footwear Insulation and Evaporative Resistance

Mitja Babič[1,*] - Jadran Lenarčič[1] - Leon Žlajpah[1] - Nigel A. S. Taylor[2] - Igor B. Mekjavić[1]
[1] Automation, Biocybernetics, and Robotics, Jožef Stefan Institute, Ljubljana, Slovenia
[2] School of Health Sciences, University of Wollongong, Australia

A sweating thermal foot manikin was developed for evaluating the thermal and evaporative resistance of footwear. The sweating thermal foot manikin can be programmed to simulate physiological patterns of conductive, convective and evaporative heat loss. The manikin can simulate the initiation and magnitude of human non-evaporative and evaporative heat loss based on core and skin temperatures. The system comprises a computer controlled system for regulating the heaters in each of the 16 segments of the foot, as well as the sweating function provided by peristaltic pumps. Each of the 16 segments is autonomous: its heating and sweating responses are controlled independently, thus the calculation of the heat exchange can also be determined for each segment separately. Results of the footwear evaluation were compared to the results obtained for identical footwear with foot manikins from other laboratories.

Keywords: human foot, thermal manikin, sweating, foot wear, physiological simulation system

0 INTRODUCTION

Selection of appropriate protective clothing and footwear in extreme conditions is very important and requires biophysical evaluation [1] to [4]. Inappropriate footwear is the main cause for freezing and non-freezing cold injury of the feet. Ensuring that footwear meets minimum biophysical standards is therefore essential in preventing cold injury. The aim of the presented work is biophysical evaluation of footwear for different climates [5] and [6].

A copper thermal manikin was build in 1940 [7] to estimate thermal characteristic of clothes and footwear. The current development of thermal manikin is focused in the development of manikins which simulates parts of the human body, e.g. foot [8] and [9], hand [10], head [11].

A manikin system for the evaluation of thermal and evaporative resistance of footwear is presented in this paper.

1 CALCULATION OF THERMAL RESISTANCE

To estimate and compare different footwear we need some type of comfort measuring tool, which includes mechanical and ergonomic comfort. The primary measurement tools for estimating thermal footwear comfort are thermal resistance per unit of surface and permeability of water vapor, or sweat evaporation.

1.1 Physical Background

We can take a body in a shape of cylinder with length L and constant intersection A (Fig. 1 a).

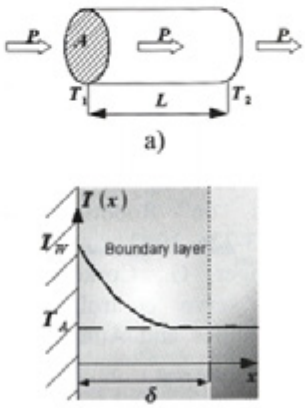

Fig. 1. *Heat transfer (see text for details)*

*Corr. Author's Address: Automation, Biocybernetics, and Robotics, Jožef Stefan Institute, Jamova cesta 39, 1000 Ljubljana, Slovenia, mitja.babic@ijs.si

Heat flux P is directly proportional to the difference of temperature T_2 - T_1 and to intersection A and inverse proportional to the length L [12]. Dependence of different materials is defined with the parameter λ (material thermal conductivity), which gives

$$P/A = -\lambda \partial T/\partial L . \quad (1)$$

Good temperature conductors (e.g. metals) have thermal conductivity values between 60 and 300 W/mK. Substances which have small values of thermal conductivity are heat insulators, e.g. air, mineral wool, etc [12]. The best thermal insulator is calm air (λ around 0.025 W/mK).

We can express the heat transfer flux from wall to air with equation (2). The temperature drop from air temperature T_A to wall temperature T_W is carried out in a thin boundary layer (Fig. 1b); the thickness of the boundary layer is δ [12].

$$P/A = \alpha(T_W - T_A) \quad (2)$$

The proportional factor α (dimension W/m^2K) is called convection ratio. It depends on physical characteristic of wall, air, and on viscosity and speed of air near the wall [12].

Equations (1) and (2) can be expressed in the form of equation (3), so that wall and boundary layer have thermal resistance $R = L/\lambda A + 1/\alpha A$. T_I is the wall inner side emperature and T_O is the air temperature at the wall outer side.

Thus the measure for estimating the footwear quality is thermal resistance R.

In the following section the basic equations

$$P = (T_I - T_O)/R \quad (3)$$

for calculating the thermal resistance per unit of surface I ($I = RA$), measure unitm^2 K /W, of each segment of manikin and the total resistance per unit on surface of the whole manikin will be carried out in the form of equation (4).

$$I = A(T_I - T_O)/P \quad (4)$$

1.2. Thermal Resistance per Unit of Surface

Thermal resistance per unit of surface for each manikin segments can be expressed as

$$I_{T,i} = \frac{(T_{S,i} - T_A)\cdot A_{M,i}}{H_{T,i}} \quad (5)$$

where $I_{T,i}$ is the segment i thermal resistance per unit of surface, $T_{S,i}$ is the segment i skin temperature, T_A is the ambient (air) temperature, $A_{M,i}$ is the area of segment i and $H_{T,i}$ is the given power to segment i (loss).

The total thermal resistance per unit of surface can be compounded from segments resistances per unit of surface

$$I_T = A_M \left(\sum_i \frac{A_{M,i}}{I_{T,i}} \right)^{-1} \quad (6)$$

where A_M is the total area of the manikin and $A_{M,i}$ is the area of segment i.

When thermal resistance per unit of surface is estimated, the air temperature is lower than skin temperature ($T_A < T_{S,i}$, $\forall i$ =1,...,16). Normally a temperature gradient around 20 °C is keept. Greater temperature gradient requires more power. The intention is to improve system resolution and accuracy.

1.3. Estimation of Evaporative Resistance per Unit of Surface in Isothermal Conditions

The evaporative resistance per unit of surface for each manikin segments can be expressed as

$$I_{E,i} = \frac{(p_i - p_A)\cdot A_{M,i}}{H_{E,i}} \quad (7)$$

where $I_{E,i}$ is the evaporative isothermal resistance per unit of surface of segment i, p_i is the partial water vapor pressure of segment i (in saturation), p_A is the ambient (air) partial vapor pressure, $A_{M,i}$ is the area of segment i and $H_{E,i}$ is the given power to segment i (loss).

The total evaporative resistance per unit of surface can be compounded from segments evaporative resistances per unit of surface

$$I_E = A_M \left(\sum_i \frac{A_{M,i}}{I_{E,i}} \right)^{-1} \quad (8)$$

where A_M is the total area of the manikin and $A_{M,i}$ is the area of segment i.

The partial saturation vapor pressure at temperature T is calculated from the empirical relation [13]

$$p_{sat}(T)=133.3\cdot\exp\left(18.6686-\frac{4030.183}{T+235}\right) \quad (9)$$

For ambient (air) partial vapor pressure we can write

$$p_A=p_{sat}(T_A)\cdot(RH_A/100), \quad (10)$$

where RH_A is the relative humidity of air. For each segment relative humidity is supposed to be RH_i = 100%, so the partial water vapor pressure for segment i is

$$p_i = p_{sat}(T_i). \quad (11)$$

Estimation of evaporative resistance per unit of surface in isothermal conditions must assure that the temperature of air is equal to skin temperature ($T_A = T_{S,i}$, $\forall i$ = 1,...,16). Under these circumstances, the heat transmission is dependent only on evaporation. It means that the given heat power $H_{E,i}$, to segment i, is equal to the process cooling evaporative power on skin.

1.4. Estimation of evaporative resistance per unit of surface in nonisothermal conditions

Evaporative resistance per unit of surface for each segment of the manikin on nonisothermal conditions can be expressed as

$$I_{S,i}=\frac{(p_i-p_A)\cdot A_{M,i}}{(H_{S,i}-H_{T,i})}=\frac{(p_i-p_A)\cdot A_{M,i}}{(H_{S,i}-\frac{(T_{S,i}-T_A)\cdot A_{M,i}}{I_{T,i}})}, \quad (12)$$

where $I_{S,i}$ is the evaporative non isothermal resistance per unit of surface of segment i, p_i is the partial water vapor pressure of segment i (in saturation), p_A is the ambient (air) partial vapor pressure , $A_{M,i}$ is the area of segment i, $T_{S,i}$ is the segment i skin temperature, T_A is the ambient (air) temperature, $I_{T,i}$ is the thermal resistance per unit of surface of segment i (previously measured) and $H_{S,i}$ is the given power to segment i (loss).

The total evaporative resistance per unit of surface can be computed from segments evaporative resistances per unit of surface

$$I_S = A_M\left(\sum_i \frac{A_{M,i}}{I_{S,i}}\right)^{-1}, \quad (13)$$

where A_M is the total area of the manikin and $A_{M,i}$ is the area of segment i.

When evaporative resistance per unit of surface in nonisothermal conditions is estimated, the air temperature is lower than skin temperature ($T_A = T_{S,i}$, $\forall i$ = 1,...,16). Normally a temperature gradient around 20 °C is keept.

2 SYSTEM DESCRIPTION

Fig. 2 shows the foot manikin system. The system is composed of a personal computer, electrical control system, sweating system and the thermal foot manikin [8] and [9]. Hereafter each part will be shortly described.

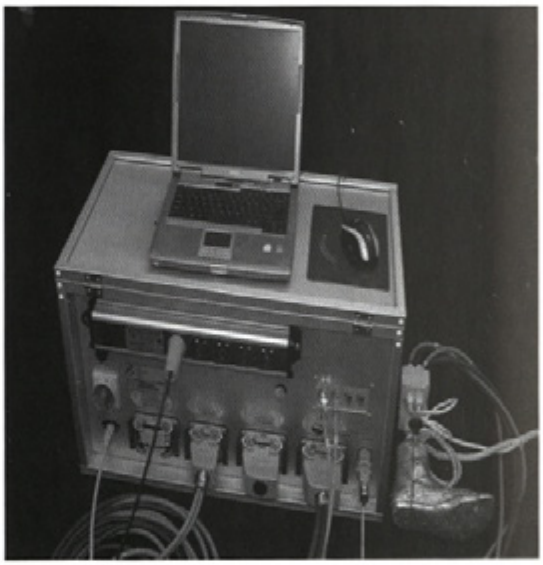

Fig. 2. *Foot manikin system*

2.1. Foot manikin

The foot manikin is composed of 16 segments. Segments are made of the alloy of silver and copper (approximately 95±5%), because silver has high thermal conductance, which causes optimal heat flux conduction from heaters to the measured material, whose resistance is measured. Also silver segments tend to have a homogeneous temperature distribution on the whole segment. Each segment has one temperature sensor, which measures the segment skin temperature $T_{S,i}$, heaters for the segment temperature control and artificial sweating glands,

which simulate the human sweating. The segment model is shown in Fig. 3a.

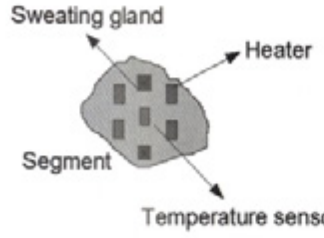

a)

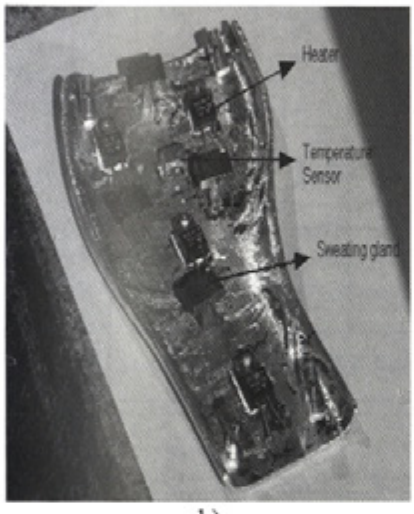

b)

Fig. 3. *a) Segment model b) Realized model of the foot sole*

The measurement and control process treats each segment as an autonomous part. Based on the temperature sensor data, the control algorithm controls the heaters in order to reach the desired segment temperature. With the control of sweating system the sweating glands wet appropriately the manikin segments. Segments thermal resistances per unit of surface calculations are based on the data obtained from the skin temperature sensors ($T_{S,i}$), the ambient (air) temperature sensor (T_A) and the control algorithm calculated power (H_i), given to the heaters.

The model part of the foot sole is shown in Fig. 3b. With the appropriate distribution of heaters and sweating glands a homogeneous sweating and heating of the whole segment is obtained.

2.2. Control system

The control system can be divided into three parts: the software part, the electronics part and the sweating system.

2.2.1 Sweating system

The sweating system is made of two peristaltic pumps, artificial sweating glands and conveyance tubes. Artificial sweating glands are mechanical elements, through which pumps transfer water to the surfaces of manikin's segments. Sweating glands are on one side connected with pumps through conveyance tubes, which supply water; holes on the other side humidify manikin's segments. Pumps are controlled by the computer via serial communication. The pumps speed can be controlled to influence the flow of water through the sweating glands, what simulates the intensity of foot sweating. The software allows starting, stopping and changing the speed of the pumps. An algorithm which simulates the foot sweating depending on the foot skin temperature is integrated in the software [14] and [15], as $v_p = f(T_{S,i},...T_{S,n})$, where $v_{p,j}$ is the pump j speed (j=1,2) , $T_{S,i}$ is the segment i skin temperature and n is the number of segments, in our case 16.

2.2.2 Electrical control system

The electrical control system consists of the power supply, National Instruments (referred as NI) PXI platform and the power output.

The base of the system is the NI PXI platform and the NI PXI control unit, which are functioning in the Microsoft Windows XP environment. The PXI platform contains the following card.

The connection between the personal computer and the NI PXI platform is made of the NI CardBus 8310 card, which together with the CardBus-to-PCI bridge, provides a transparent link where all PXI modules appear as if they are PCI boards within the computer itself. This allows an easy communication with the selected PXI module.

Two NI 4351 cards acquire data from temperature sensors. The properties of the card are high accuracy, resolution and big CMRR factor (CMRR- common mode rejection ratio).

The foot manikin has 16 Pt 1000 resistance temperature detectors, which are supplied with current source of 1mA. The length of the connection cables form the foot manikin to the controller is more then 3m, so in order to increase the measurement accuracy reduction of cables length is needed. For that reason a three wire connection is used to connect the temperature detectors (Fig. 4a). In this configuration only wire resistance R_{L1} adds error to the measurement.

The NI 6221 card has digital inputs and outputs. With this card we control opto couplers, which turn the heaters on and off (Fig. 4b). For heating segments we use power resistors RTO 20, which principal property is that power-temperature characteristic negligible change with temperature change.

The last NI PXI card is a serial communication card. This card has four serial ports which are used to control the pumps.

NI PXI supports various environments, between them also Microsoft Windows XP, which is used to build our software system.

2.2.3 Software environment

The manikin control system was built in the C++ programming language. Fig. 5 shows the measurement flow chart in real time. The system user can communicate with the software and hardware system in the graphical user interface. At the beginning the user has to define and configure the measurement. After the measurement starts the software communicates with the hardware through the NI PXI platform. From the acquired temperature sensors data and previously defined temperature references, the software algorithm controls the heaters. The software algorithm also controls through the NI PXI platform the pumps, which control the sweating glands in order to reach the desired sweating of the foot. After every sampling time the control process is repeated. The measured data are calculated and displayed on-line. The measurement stops automatically when some predefined reference condition is reached or the process is stopped manually.

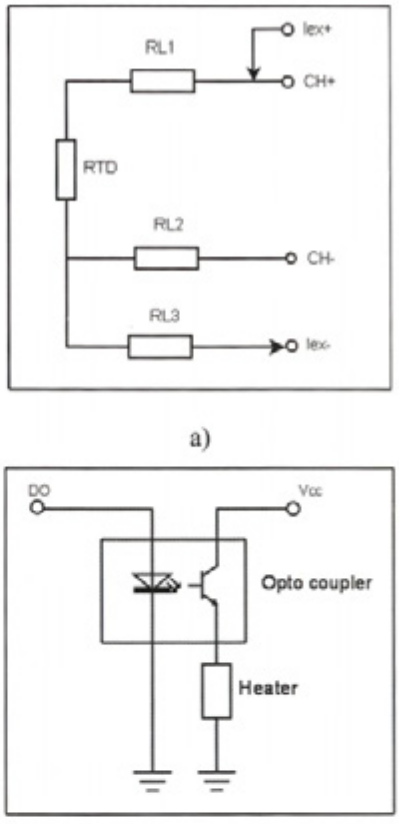

Fig .4. *a) Temperature measurement b) Power output*

2.2.4 Control algorithm

Fig. 6 shows the flow chart of the control algorithm for one segment.

The control algorithm is composed of 16 PID regulators with anti-windup protection, which control 16 pulse width modulators (PWM) for control of the segment heaters. A proportional-integral-derivative (PID) control algorithm is given with equation (14).

$$u(t) = K_p e_p(t) + K_I \int e_I(t)\, dt + K_D \frac{de_v(t)}{dt} \qquad (14)$$

PID is made with the parallel combination of P, I and D term. With the appropriate parameters tuning we influence the system response (P, D) and the steady-state error (I). Computer simulation in Matlab-Simulink

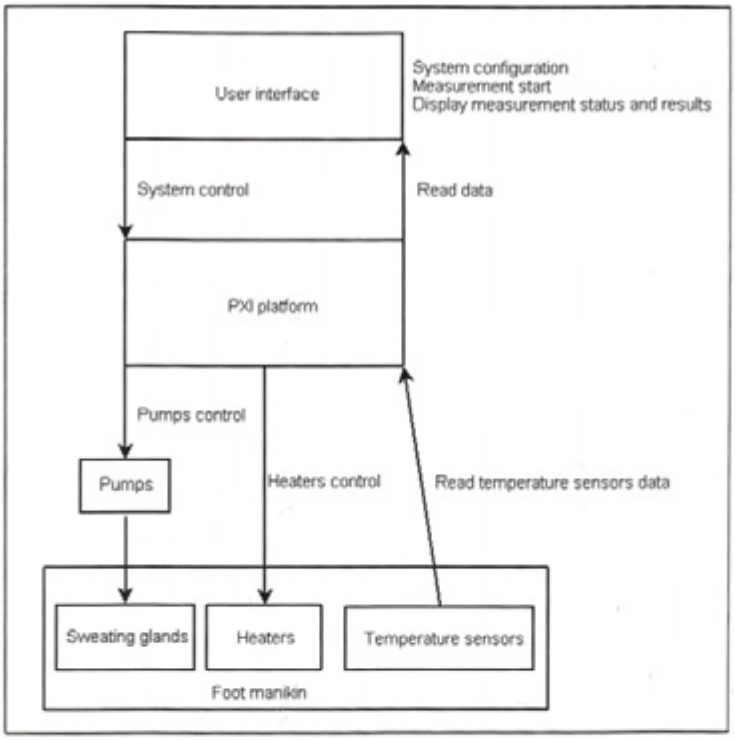

Fig. 5. *Chart of the measurement process*

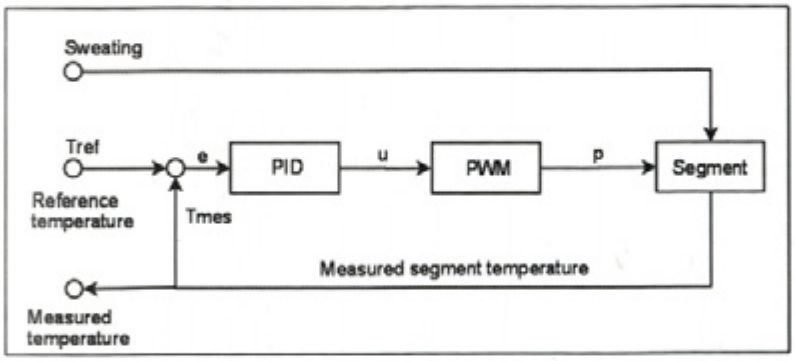

Fig. 6. *Control algorithm*

gives as the initial approximate values of *P, I, D* parameters. Finally, the parameters were fine tuned on the real system. We reach settling time lower than 3min and steady-state error lower than $\Delta T < \pm 0.5°C$.

On windup the control system goes in saturation during regulation, so the error is decreasing more slowly, as if saturation would not be present. The basic idea of anti-windup is to find out when the control system goes in saturation. At the time this happens it is necessary to stop the integration of the regulator I term, or respectively influence the I term in the way that the regulator will bring the control system near the saturation limit. Because the regulator is controlling the heaters with pulse width modulation, which has limit values between zero and one, it is necessary to adapt the control algorithm to these limits.

It is important to emphasize that the whole control algorithm is made programmatically, so the regulator is discretized and works with sampling time $T_s = 5s$.

Fig. 7. *Control system algorithm*

Heaters are controlled with Pulse Width Modulation (*PWM*). Therefore the regulated heater power is directly proportional to the signal duty cycle

$$H_{\mathrm{i}} = H_{\mathrm{max,i}} \cdot \Delta t_{\mathrm{ON,i}} \,, \qquad (15)$$

where $H_{\mathrm{max,i}}$ is the heater maximum power and 5s is the signal duty cycle.

In our system program timers are used for the generation of PWM signals. The standard timers accuracy is around Δt_{TIM} = (10 to 15) ms, with the use of multimedia timers the resolution can reach a limit of Δt_{TIM} = 1 ms. Because the sample time period is TS = 5 s, the minimum resolution of the PWM signal can be

$$\Delta PWM = \frac{\Delta t_{\mathrm{TIM}}}{T_{\mathrm{S}}} = 2 \cdot 10^{-4},$$

or expressed in heater power

$$H_{\mathrm{i}} = \frac{V_{\mathrm{CC}}}{R_{\mathrm{H,i}}} \Delta PWM_{\mathrm{i}} \approx \frac{(24\,\mathrm{V})^2}{45\,\Omega} \cdot 2 \cdot 10^{-4} = 2.56\ \mathrm{mW},$$

where V_{CC} is the power supply voltage and $R_{\mathrm{H,i}}$ is the segment i heater resistance.

Beside the closed-loop control regulation the system also allows open-loop control regulation, which means constant heater power of the segment regardless to the segment temperature. From the given desired power of segment *i*, H_{i}, the system calculate the PWM signal duty cycle:

$$\Delta t_{\mathrm{ON,i}} = \frac{H_{\mathrm{i}}}{H_{\mathrm{max,i}}},$$

which controls heaters. With this method we can find out which is the steady state of the skin temperature at constant heating power for given footwear.

The sweating system is controlled with an open-loop algorithm. The pumps can be turned on or off. With pumps speed control influence the flow of water through the artificial sweating glands, what simulate the human foot sweating. If we want to change the flow of water through each sweating gland, we can achieve this with changing the tube diameter.

Fig. 7 shows the flow chart of the control algorithm. After the regulation type is chosen (closed-loop or open-loop) the selected

algorithm is repeated in sampling time T_s = 5s. After some reference condition is reached, the measurement stops.

3 MEASUREMENT RESULTS

3.1. System Check Up

Some reference tests have been done to check the system behavior and to compare our manikin with other manikins. For this reason we did four tests with bare foot, sock, rubber boot and winter boot. We put the manikin in a climatic chamber on temperature T_A = 15°C, relative humidity RH_A = 50%, without wind. Dry test have been done with foot reference temperature set to T_F = 35°C. Test duration was 90 min, each test was repeated twice. The manikin result tests were checked and compared to the results from other laboratories manikins, which results were described by Kuklane et al. [16]. The test results are shown in Table 1.

Table 1 show that the thermal resistance per unit of surface increases, as expected. Values increase with more thermally insulated footwear. The values are near the mean values of other manikin's tests described in [16]. The results for bare foot and sock are near the mean values in [16], meanwhile for rubber boot and winter boot the values are lower than the expected values. The main reason was that the wear did not fit the foot well, which cause lose of power heat. All tests were repeated twice and the differences in the results were around ΔI = ±0.005 m²K/W, which is the system accuracy and depends on the accuracy of sensors, program timers, etc.

3.2. Wind influence

Some test has been done to study the response of the foot manikin in the presence of wind. Simulation of wind was carried out with a fan. The results are shown in Fig. 8.

Fig. 8 show that the thermal resistance per unit of surface decreases, because the wind is cooling the foot and the regulator needs to increase the given power, to keep the foot on the same temperature.

Time course of relative measurement values for one segment (segment 5) is depicted in Fig. 8c (Tsrel-temperature skin, Irel-thermal resistance per unit of surface, HArel-heat flux per unit of surface).

Total thermal resistance per unit of surface without wind is

$$\Delta I_{NW} = 0.107 \text{ m}^2\text{K/W}$$

and with wind is

$$\Delta I_{W} = 0.067 \text{ m}^2\text{K/W}.$$

3.3. Influence of wind and sweating

The last test shows the influence of wind and sweating on the foot with sock. The measurement results are shown in Fig. 9.

Fig. 9 shows that sweating is cooling and wetting the sock, what results in the need of more power from the system to maintain the reference temperature and causes the thermal resistance per unit of surface to decrease.

Time course of relative measurement values for one segment (segment 5) is depicted in Fig. 9c (Tsrel-temperature skin, Irel-thermal resistance per unit of surface, HArel-heat flux per unit of surface).

Total thermal resistance per unit of surface are

$\Delta I_{PNW} = 0.065$ m²K/W for pumps without wind,

$\Delta I_{PW} = 0.039$ m²K/W for pumps with wind and

$\Delta I_{PNW} = 0.061$ m²K/W for pumps without wind.

Table 1. *Comparison of thermal resistance per unit of surface derived for bare foot, sock, rubber boot and winter boot. Results are compared to those reported by Kuklane et. al. (2005)*

Footwear	Measured I_M m²K/W	Reference I_R m²K/W
Bare foot	0.0843	0.090
Sock	0.112	0.120
Rubber boot	0.139	0.170
Winter boot	0.189	0.225

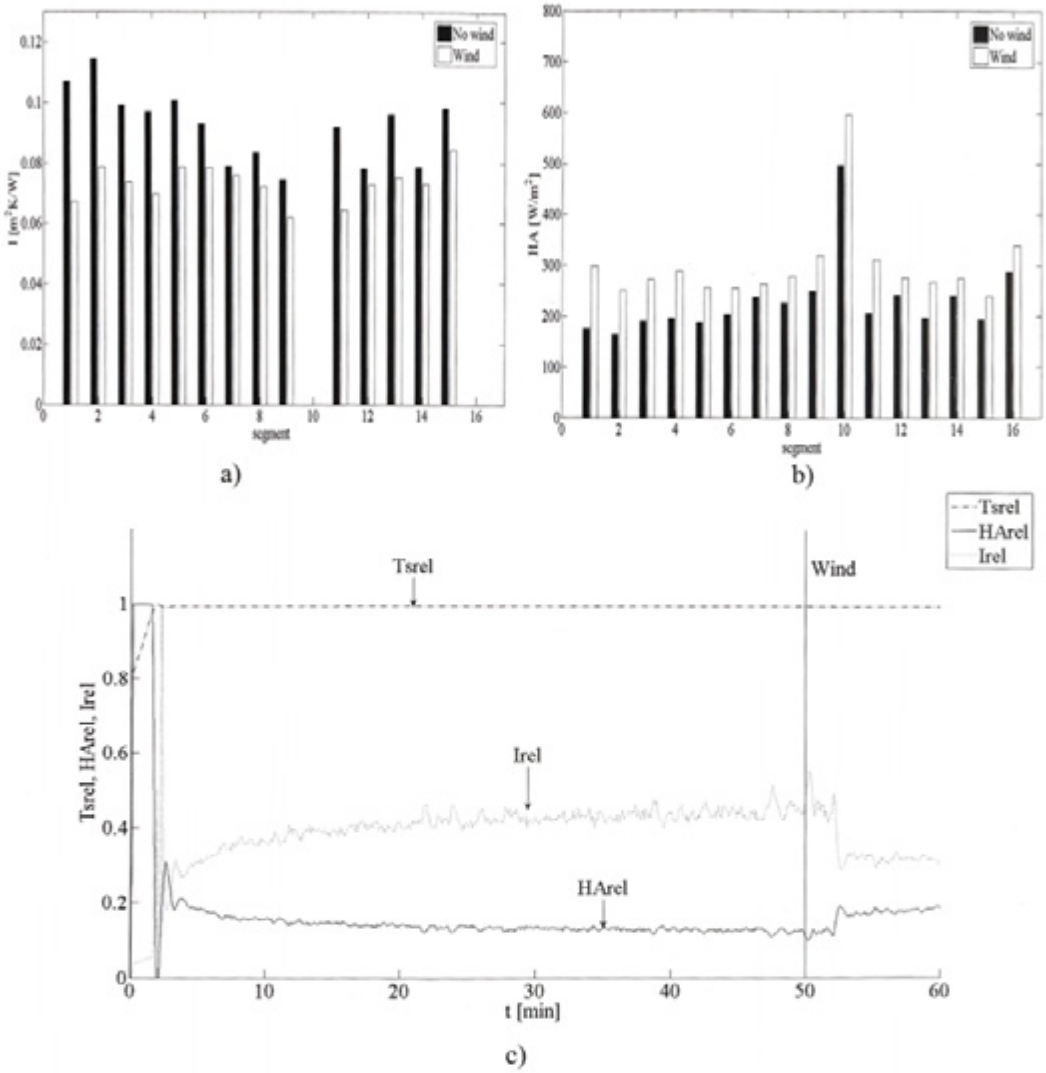

Fig. 8. *Influence of wind on thermal resistance per unit of surface (sock) thermal resistance per unit of surface b) heat flux per unit of surface c) time course of relative measurement values*

3.4. Studying the characteristics with infra-red camera

Fig. 10 shows two pictures obtained with infra-red camera when the foot is heated from 15°C to 35°C. Fig. 10a shows the foot at the temperature near 30°C, in Fig. 10b the temperature is around 35°C, which is the steady state.

Fig. 10 shows that the segments are heating homogenously. Leg is filled with silicone rubber inside, which mechanically connects segments together. Silicone rubber is transferring warmth from one segment to another partially (dark lines between segments Fig. 10b). For an accurate analysis the system could be treat as a multivariable system, what could increase the difficulty of system analysis, control and calculations. The construction of our next manikins will be made in such a way that segments will be connected together mechanically with some holders. So they will be inside hollow, what will presumably reduce the heat transfer between segments.

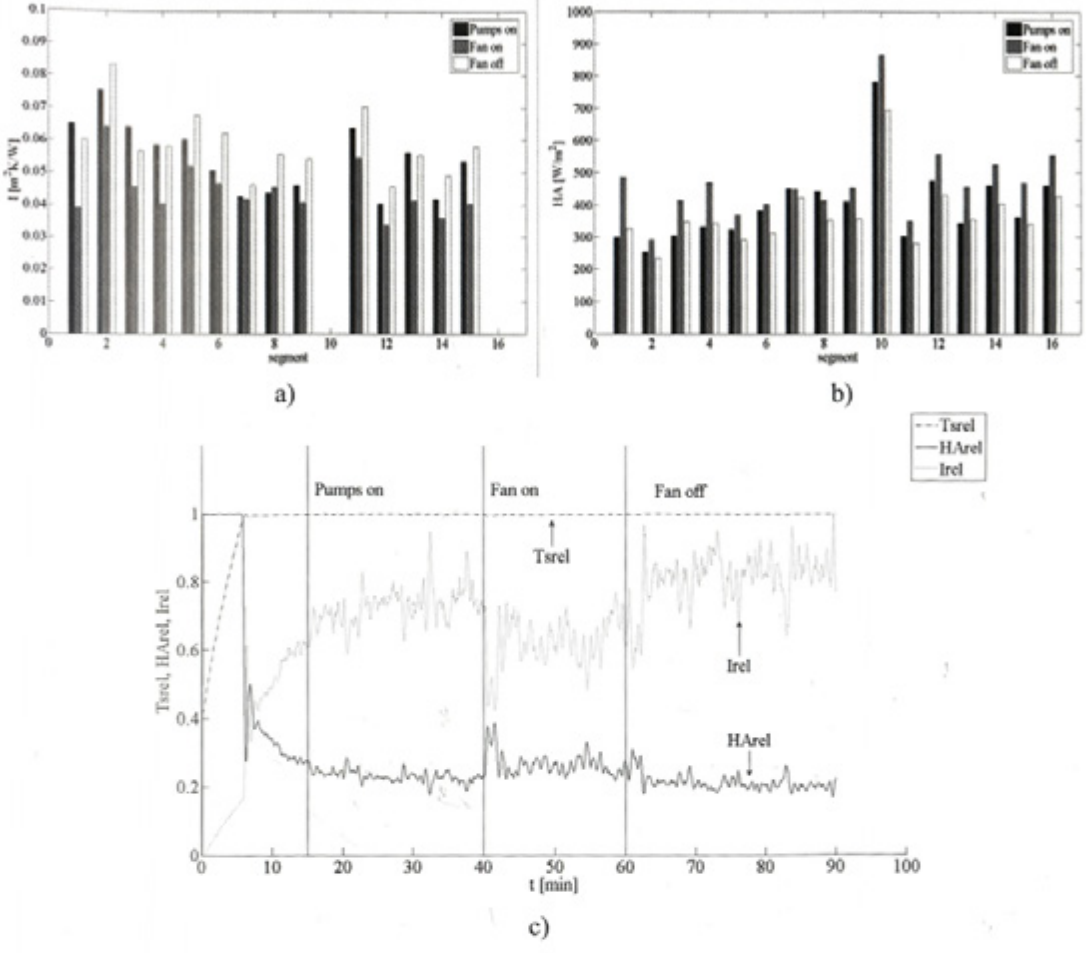

Fig. 9. *Influence of wind and sweating (sock)*
a) thermal resistance per unit of surface b) heat flux per unit of surface c) time course of relative measurement values

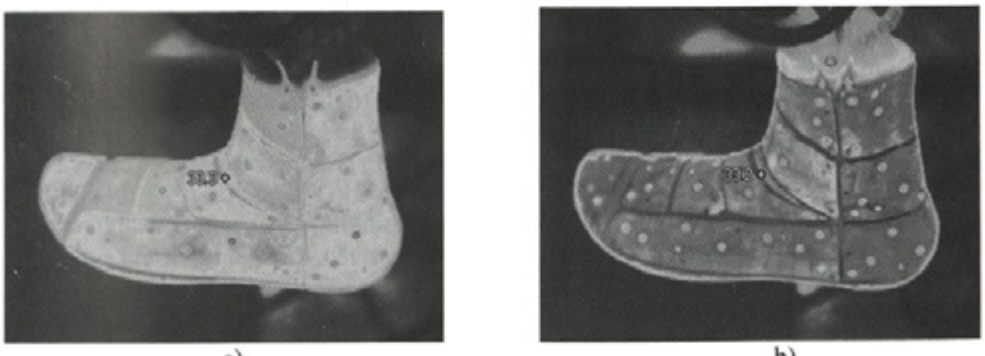

Fig. 10. *Infra-red thermograms of the foot manikin at a) 30°C and b) 35°C*

4 CONCLUSION

A device for footwear quality estimation and physiologic simulation of the human foot was presented. The system calculates the thermal and evaporative resistance to estimate the quality of the footwear. The manikin can simulate thermal behaviors of the foot and sweating of the foot. There are many built-in functions for control of the foot heating and sweating.

The device construction, control system and the thermal resistance measurement are presented. Sixteen segments compose the foot manikin. Each segment is an autonomous part, in the sense of construction, control and calculation. The goal of using segments is that with segments we can test the quality of each part of the footwear, what is the base information for the manufacturer and user.

The test results are comparable with manikins from other laboratories.

5 REFERENCES

[1] Fourt L., Hollies N.R. (1970), Clothing. Comfort and Function. Marcell Dekker: New York.

[2] Hollies N.R., Goldman R.F. (1977), Clothing Comfort. Interaction of Thermal, Ventilation, Construction and Assessment Factors. Ann Arbor Science Publishers Inc.:Ann Arbor, Michigan.

[3] Newburgh L.H. (1968), Physiology of Heat Regulation and the Science of Clothing. Hafner Publishing Co.: New York.

[4] EN344 (1992), Requirements and test methods for safety, protective and occupational footwear for professional use [European Standard]. Brussels: European Committee for Standardization.

[5] Mekjavić I. B., Tomšič M., Rodman S. (2002), Determination of thermal insulation of hiking shoes. Medicinski razgledi 41, p. 183 - 186.

[6] Santee W.R. and T.L. Endrusick (1988), Biophysical evaluation of footwear for cold-weather climates. Aviation, Space and Environmental Medicine 59, p.178-182.

[7] Holmér I. (2004), Thermal manikin history and applications. European Journal of Applied Physiology, vol.92, no.6, p.614-618(5).

[8] Mekjavić I. B., Vrhovec B., Tomšič, M., Lenart B. (2005), Sistem za ovrednotenje dinamične toplotne izolacije obutve, (IJS delovno poročilo, 9273).

[9] Tomšič M. (2004), Izdelava modela noge za merjenja toplotne izolacije, (IJS delovno poročilo, 9066).

[10] Kuklane K., Nilsson H., Holmer I., Liu X. (1997), Methods for handwear, footwear and headgear evaluation. Proceedings of a European seminar on manikin testing. National Institute for Working Life, Stockhom, Sweden, February 1997.

[11] Bruhwiler P. A., Ducas C., Huber R., Bishop P.A. (2004), Bicycle helmet ventilation and comfort angle dependence. Eur. J. Appl. Physiol., 92, p. 698-701.

[12] Rudolf K. (1989). Visokošolska fizika I.del, DZS, Ljubljana.

[13] Buck, A. L. (1981), New equations for computing vapor pressure and enhancement factor, J. Appl. Meteorol., 20, p. 1527-1532.

[14] Taylor N. A. S., Caldwell J. N., Mekjavić I. B. (2006), The sweating foot : local differences in sweat secretion during exercise-induced hyperthermia. Aviat. Space Environ. Med., 77, p. 1020-1027.

[15] Machado-Moreira C.A., Smith F.M., Van den Heuvel A. M. J., Mekjavić I. B., Taylor N. A. S. (2008). Sweat secretion from the torso during passively-induced and exercise-related hyperthermia. Eur. J. Appl. Physiol. In press.

[16] Kuklane K., Holmér I., Anttonen H., Burke R., Doughty P., Endrusick T., Hellsten M., Shen Y., Uedelhoven W. (2005), Interlaboratory tests on thermal foot models. In: Tochihara, Y. and Ohnaka, T. (editors). Environmental Ergonomics - The Ergonomics of Human Comfort, Health, and Performance in the Thermal Environment.